

Anomalous oscillatory magnetoresistance in superconductors

Milind N. Kunchur* and Charles L. Dean

Department of Physics and Astronomy, University of South Carolina, Columbia, South Carolina 29208, USA

Boris I. Ivlev

Instituto de Física, Universidad Autónoma de San Luis Potosí, San Luis Potosí, 78000, Mexico

(Received 25 September 2015; revised manuscript received 30 June 2016; published 4 August 2016)

We report oscillatory magnetoresistance in various superconducting films, with a magnetic-field period $\Delta B \sim 0.1$ T that is essentially independent of sample dimensions, temperature, transport current, and the magnitude and orientation of the magnetic field, including magnetic fields oriented parallel to the film plane. The characteristics of these oscillations seem hard to reconcile with previously established mechanisms for oscillations in magnetoresistance, suggesting the possibility of another type of physical origin.

DOI: [10.1103/PhysRevB.94.054504](https://doi.org/10.1103/PhysRevB.94.054504)**I. INTRODUCTION AND BACKGROUND**

The formation of the superconducting state involves a delicate congruence between the parameters of the electronic structure and the interactions between the charge carriers and excitations in the solid. Minute alterations in any of these conditions can sensitively alter the superconducting state as reflected by its transition temperature T_c and its resistance R in the dissipative regime. R decreases when the superconducting component strengthens and provides a sensitive probe of small changes in the underlying electronic structure. Arising from flux vortex motion, fluctuations, and percolation between resistive and zero-resistance regions, R is typically a monotonically rising function of T , magnetic field B , and transport electric current I . In particular, the magnetoresistance is usually positive; however, certain circumstances can lead to an oscillatory magnetoresistance (OMR).

The most straightforward source of OMR in superconductors is related to fluxoid quantization and the formation of Abrikosov or Josephson flux vortices; this behavior is well exemplified by Josephson-junction (JJ) arrays, regularly patterned hole or wire networks, and other mesoscopic and multiply connected systems [1–24]. For this class of effects, the OMR period is $\Delta B \approx \Phi_0/S$, where S is the effective cross sectional area facing the magnetic field that the flux links to, and $\Phi_0 = h/2e$ is the flux quantum. Because of the geometrical basis of the period, such oscillations can be expected to have a period that is naturally independent of T , B , and I . However, ΔB would still depend on the orientation of B since the projection of the geometrical area onto the plane perpendicular to B , and hence S , will change with angle.

What is surprising is that sometimes systems that have not been purposely engineered to have regularly arranged structures also show remarkably periodic OMR. This has been previously reported by other groups in the literature and is further explored in the present experiments. Here we present evidence and arguments that the usual explanations offered for such OMR—based on granularity and inhomogeneity causing vortex and junction related effects—are probably not valid

and some potentially different mechanism might underlie the observed OMR.

In the work by Herzog *et al.* [25] on granular tin wires (grown by thermal evaporation onto cryogenically cooled substrates), they observed some OMR which they tentatively compared to the behavior JJ arrays [26]. In a granular superconductor, one would expect that the grain sizes and areas of loops (formed randomly through the coupling of grains) would have spreads in their values so that there would not be a single pronounced period because of averaging. It might be expected that if the film is patterned into a sufficiently tiny bridge, this volume may enclose so few grains that the limited averaging may allow at least some crude oscillatory behavior to survive. This was the argument put forth in Ref. [25] and they indeed found that although their 2D granular films do not show OMR, their very tiny nanobridges (of thicknesses $d \sim 100$ nm, widths $w = 110$ – 200 nm, and lengths $l = 1$ – 4 μm) did show it. In that work, consistent with a random granular system, the oscillations had a weak amplitude and appeared to be a superposition of multiple periods (the lowest common multiple of these periods appears to be $\lesssim 0.4$ T).

However, even nongranular systems show OMR, such as observed by Wang *et al.* in nanobridges patterned from high-purity single-crystalline Pb films grown by low-temperature molecular beam epitaxy (MBE) [27]. Their samples 3 and 4, which showed low- B OMR similar to ours, had dimensions of $d \sim 8$ nm, $w \approx 300$ nm, and $l = 2$ and 10 μm . The OMR periods were $\Delta B = 0.13$ T and 0.18 T, respectively. These authors do not claim to know the mechanism for their oscillations in their samples 3 and 4, although they hint at the possibility of ringlike structures along the lines of the tentative explanation offered in Ref. [25].

Johansson *et al.* [28] studied superconducting wires of amorphous indium-oxide made by electron-beam evaporation of a:InO onto a WS_2 nanowire suspended across a narrow gap in a substrate. Their sample 99Nb shows an OMR with a strong fundamental period of $\Delta B = 0.12$ T; this sample has dimensions of $d \sim 30$ nm, $w \approx 120$ nm, and $l = 3.4$ μm .

All of these previous works were on wires of very small cross section [$\sim (1$ – $10) \times 10^{-15}$ m^2], focusing mainly on low-temperature conventional superconducting systems (e.g., Sn, Pb, and InO), and measured with the magnetic field oriented perpendicular to the film plane (B^\perp). But what emerges

*Corresponding author: kunchur@sc.edu; <http://www.physics.sc.edu/kunchur>

from these results is that despite the diversity of materials, methods of preparations, and differences in morphology and dimensions, all have OMR fundamental periods within the narrow range of 0.12–0.18 T.

In the present work we investigated OMR in high-temperature cuprate superconducting films, with bridges of much more extended sizes (cross sections as large as 1×10^{-11} , four orders of magnitude larger than the previous nanobridges), and have also studied the behavior for magnetic fields parallel to the film plane (B^{\parallel}), in addition to B^{\perp} . We found that the oscillation period ΔB is independent of the orientation of B . While the main focus of the present work is on films of the electron-doped infinite-layer $\text{Sr}_{1-x}\text{La}_x\text{CuO}_2$ superconductor, we have also observed the oscillations in another electron-doped cuprate $\text{Nd}_{2-x}\text{Ce}_x\text{CuO}_4$, in a hole doped cuprate $\text{Y}_1\text{Ba}_2\text{Cu}_3\text{O}_7$, in a conventional superconductor NbTiN, and in the interface between a topological insulator (Bi_2Te_3) and a chalcogenide (FeTe). Our observed OMR covered temperatures ranging 4–74 K and sample dimensions covering $d = 7\text{--}250$ nm, $w = 4\text{--}50$ μm , and $l = 70\text{--}2000$ μm . Despite the large ranges in parameters and dimensions in the samples we studied, our OMR periods remain narrowly clustered within the range of $\Delta B = 0.11\text{--}0.15$ T, comparable to the $\Delta B = 0.12, 0.13,$ and 0.18 T observed in the aforementioned work on low- T_c systems. This relative constancy of period across such an enormous range of parameters, dimensions, and field orientations makes explanations based on fluxoid quantization and vortices implausible. As we show below, other known mechanisms of OMR (based on Fermi surface geometry, spatial modulations in the superconducting state, etc.) are also incompatible with this OMR phenomenon, thus pointing to the possibility of a fundamentally new underlying mechanism.

II. EXPERIMENTAL DETAILS

The main measurements in this study are on c -axis-oriented epitaxial thin films of $\text{Sr}_{0.88}\text{La}_{0.12}\text{CuO}_2$ (SLCO) deposited on heated KTaO_3 substrates by rf magnetron sputtering followed by an oxygen reduction step. X-ray diffraction spectra show the films to be epitaxial and highly c -axis-oriented (with a mosaicity of 0.1°), and single phase with undetectable ($<0.1\%$) impurity phases. SLCO sample A had the following parameters: thickness $d = 31$ nm, width $w = 13.6$ μm , length $l = 512$ μm , midpoint transition temperature $T_c = 23.3$, and a transition width (10%–90% of normal resistance) of $\Delta T_c \approx 2.5$ K. Sample B had $d = 61$ nm, $w = 4$ μm , $l = 100$ μm , $T_c = 26.5$ K, and $\Delta T_c \approx 2.5$ K. Also included in this study is a c -axis-oriented epitaxial thin film of $\text{Y}_1\text{Ba}_2\text{Cu}_3\text{O}_7$ (YBCO) deposited on a SrTiO_3 substrate by the pulsed-laser-deposition process, with $d = 50$ nm, $w = 4$ μm , $l = 70$ μm , $T_c = 78.6$ K, and $\Delta T_c \approx 9$ K; and a NbTiN film sputtered onto a Si wafer with a 400 nm thick oxide layer, with $d = 125$ nm, $w = 8$ μm , $l = 115$ μm , $T_c = 10.46$ K, and $\Delta T_c \approx 0.5$ K. SLCO sample A was a four-probe bridge with a straight current path [Fig. 1(b)] patterned with contact photolithography followed by wet etching. SLCO sample B and the YBCO and NbTiN samples were four-probe bridges with a folded current path [as shown in Fig. 1(a)] and were patterned by projection photolithography and argon-ion milling. The geometries, dimensions, and lead



FIG. 1. Schematics of sample patterns (not to scale) and lead arrangements. Actual voltage (V) and current (I) contacts are far removed (>1 mm) from the bridges. (a) Four-probe bridge with a folded current path. (b) Four-probe bridge with a straight through current path and voltage contacts on one side.

arrangements are quite different for the two SLCO samples, making it unlikely that a particular lead arrangement or overall geometry is at the root of the observed oscillations. Contacts were made by smearing indium onto contact areas that are far removed (>1 mm) from the bridge and then pressing down copper wires with indium pads. In the case of the SLCO samples, gold dots were deposited in the contact areas prior to the indium treatment. Contact resistances are <1 Ω (much lower than the actual resistance of the bridge being measured).

The cuprate samples were characterized by broad transitions, which facilitates the observation of the OMR since the sample remains resistive but well below normal resistance for the B field range over which the OMR occurs. The NbTiN sample has a relatively sharp transition but shows OMR if the current is low enough.

The cryostat was a Cryomech PT405 pulsed-tube closed-cycle cryocooler, fitted with a 1.2 T GMW 3475-50 water-cooled copper electromagnet. A nonsuperconducting electromagnet is particularly suited for measurements in low fields with numerous closely spaced field steps; a superconducting magnet can add complexity, especially if it goes in and out of persistent mode for every data point. The cryocooler’s cold head is far removed from the magnet, with a 22 cm long copper rod protruding from the second-stage heat station into the magnet poles; this eliminates changes in cooling power and temperature that may be caused by the magnetic field. The sample along with a calibrated cernox sensor (which serves as the primary thermometer) and a diode temperature sensor are mounted in close proximity at the end of this copper rod (an additional diode sensor on the second-stage heat station serves as a tertiary indicator). A Hall sensor provides the primary measurement of B , and the current supplied to the electromagnet serves as a secondary indicator of B . The standard active temperature controller was disconnected, since it can produce oscillations in T and add electrical noise. To further avoid temperature variations during the measurement of each $R(B)$ curve, all measurements were conducted at a fixed phase point of the compressor cycle. These special measures and redundancies provided for unusually clean and stable conditions, and highly reliable measurements of B and T for each data point. The reliability of this system’s measurement of R , and stability of T over time and against changes in B was extensively checked with resistors as “test samples” and through the continuous monitoring of all three thermometers. Figure 2 shows the temperature indicated by the cernox thermometer along with a ruthenium-oxide (RuO_2)

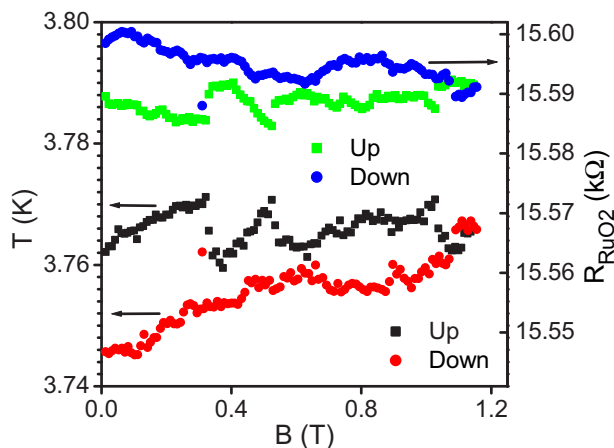


FIG. 2. Measurements of the temperature, as indicated by the cernox thermometer, and a ruthenium oxide resistor (mounted as a test sample) show close tracking between temperatures at the sample and thermometer locations and a total temperature variation over time and magnetic-field change of $\lesssim 20$ mK.

resistor mounted as a test sample. Like the cernox, RuO_2 also has a negative temperature coefficient of resistance and a very slightly negative magnetoresistance. It can be seen that, despite occasional small jumps, long-term drifts, and any possible B dependent shifts, T stays within a $\lesssim 20$ mK window over the duration of the entire curve, with a short-term stability of ~ 1 mK.

Except where noted, the $R(B)$ data represent four-probe resistance measurements at a constant dc current of $I = 12.8 \mu\text{A}$, taken with current-direction-reversed averaging, i.e., $R = (V^+ - V^-)/(I^+ - I^-)$, the ratio of the difference of the forward and reverse voltages to the corresponding difference in the forward and reverse currents. All data are completely reversible with respect to changes in I , T , and B . All data also lie in the ohmic response regime (except for the one set of variable- I curves). To minimize electrical noise, the dc current source consisted simply of an alkaline battery and a large series resistor, serving as a ballast to hold the current constant. (A Hewlett Packard 5532A dc power supply replaced the battery for the variable- I curves.) Except where noted, the sample voltage was measured with a Keithley model 2182A nanovoltmeter and other voltages were measured with Keithley model 2000 multimeters, with each quantity averaged over ~ 30 readings (individual readings had integration times of 17 ms). The single confirmatory $R(B)$ curve measured with pulsed signals utilized a Wavetek model 801 pulse generator, in-house built electronics, and a LeCroy LT 322 digital storage oscilloscope.

Despite the seemingly long description of the experimental setup, we would like to emphasize that when you come right down to it, our apparatus is actually very simple and least subject to interpretation compared to a commercial automated turn-key measurement system as follows. (1) Our current source for most of the data is simply a battery with a series resistor, (2) the magnet is not superconducting but a copper-wire electromagnet with an iron core and you can obtain the B value also from the magnet current besides the Hall probe, (3) instead of the constantly varying power

supplied by a traditional automatic temperature controller, we have driven the control heater with a nonfluctuating stable dc voltage resulting in a constant temperature since the cooling power remains essentially constant, and (4) some of the data were measured entirely by hand without the use of a computer automated data acquisition. Thus it will become clear from the extensive tests described below that the observations are free from experimental artifacts.

III. DATA AND RESULTS

Figure 3(a) shows $R(B)$ curves for various fixed T for the B^\perp orientation ($B \perp$ film plane) in SLCO sample A. There are pronounced oscillations over wide ranges of T and R , superimposed on a steadily rising background magnetoresistance that follows the $R/R_n \sim B/B_{c2}$ flux-flow relation [this linearity is more conspicuous on the linear-linear graph shown in Fig. 4(a)]. The oscillations are not symmetric but have sharper minima in $R(B)$, which we will denote by B_X .

A graph of B_X vs count is very linear [Fig. 4(b)] indicating a high periodicity, and the slope of the straight-line fit yields a period of $\Delta B = 0.149 \pm 0.004$ T independent of T ; a fast Fourier transform (FFT) of $R(B)$ produces the value $\Delta B = 0.154 \pm 0.008$ T. The oscillations are strongest in the $B < 0.5$ T range and appear to fade at higher B . Comparing

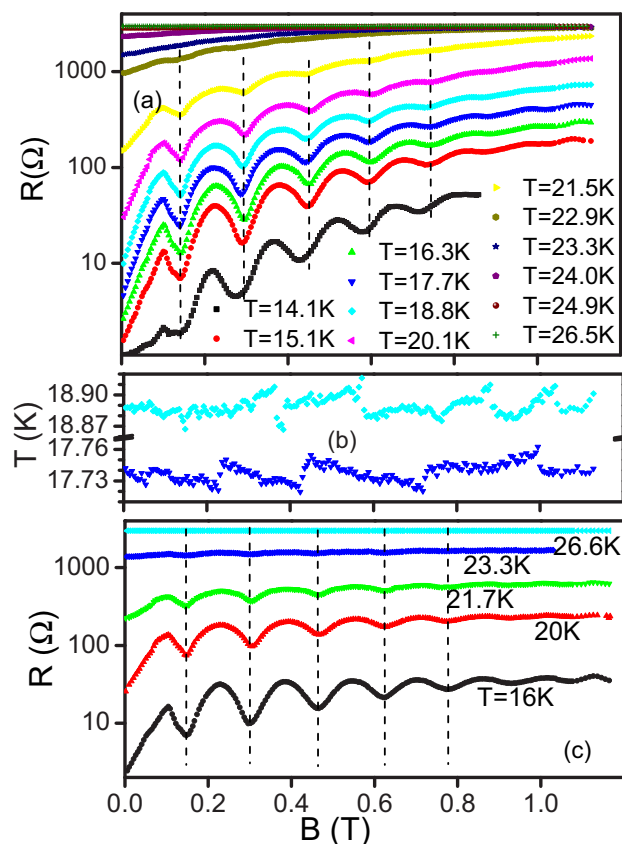


FIG. 3. (a) B^\perp magnetoresistance curves in SLCO sample A for various temperatures. Vertical dashed lines pass through the minima B_X . (b) Temperature variations for the “17.7 K” and “18.8 K” resistance curves in above panel. (c) B^\parallel magnetoresistance curves in same sample.

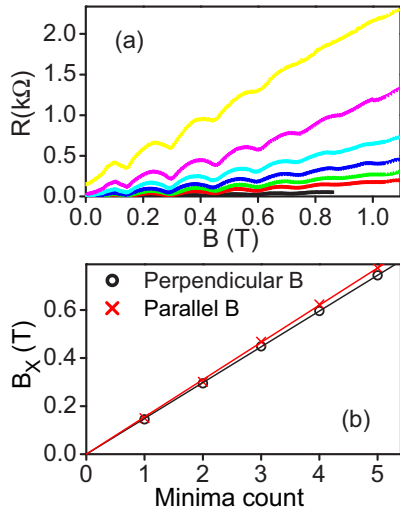


FIG. 4. (a) Linear-linear plot of $R(B)$ curves from Fig. 3(a) (SLCO sample A in B^\perp). Although the lower T curves are now more compressed, this graph better displays the $R \propto B$ general response under the oscillations. The slopes closely reflect free flux flow, i.e., $dR/dB \approx R_n/B_{c2}$. (b) Magnetic fields corresponding to minima in $R(B)$ graphs for perpendicular and parallel fields. The slopes of the straight-line fits yield a period of $\Delta B = 0.149 \pm 0.0004$ T and $\Delta B = 0.155 \pm 0.0008$ T for B^\perp and B^\parallel , respectively.

curves at different T , the oscillations get weaker and disappear as the normal state is approached, indicating that they are a feature related to the superconducting state and that the normal state magnetoresistance is itself not oscillatory. In fact, the effect seems to be most prominent where $R \ll R_n$, i.e., in the foot of the resistive transition.

The amplitude of the oscillations is so large (e.g., $\Delta R = 78 \Omega$, minimum to maximum, for the 17.7 K curve) that it cannot possibly arise from a variation in T : the $dT/dR \approx 0.025$ K/ Ω would imply a $\Delta T = 1.9$ K, which is drastically higher than the ± 15 mK maximum variation of the measured temperatures shown in Fig. 3(b).

Figure 3(c) shows similar oscillatory $R(B)$ curves for the B^\parallel orientation ($B \parallel$ film plane), which have a comparable fractional amplitude superimposed on a less steep background magnetoresistance (reflecting the much higher B_{c2} and lower flux mobility for B^\parallel). The periodicity of $\Delta B = 0.155 \pm 0.008$ T is the same as for B^\perp within error, which calls into question any explanation of the phenomenon based on vortices and fluxoid quantization.

Figure 5(a) shows that the oscillations vanish as I is increased, indicating that some delicate property of the superconducting transition is needed; this action is similar to the effect of increasing T seen in Fig. 3(a). These observations establish that the oscillations are not an artifact of the voltage measurement, which is indifferent to the I , B , and T of the sample. Could it be that there is something special happening in the apparatus around $T \sim 20$ K and $R \sim 100 \Omega$, which serendipitously coincides with the transition in this superconductor? No, because we have seen these oscillations in a variety of systems spanning the ranges $T = 4\text{--}74$ K and $R = 0.01\text{--}1000 \Omega$, with fractional resistance amplitudes ranging from zero to $>50\%$. Also of significance is the fact

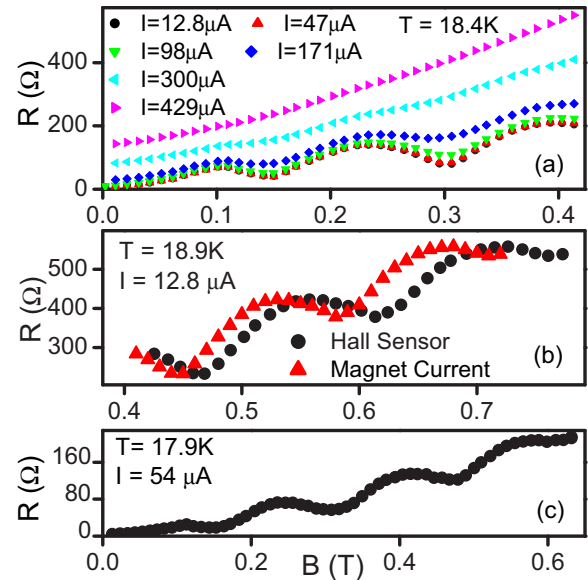


FIG. 5. (a) Magnetoresistance curves at various dc currents. Oscillations are most prominent at low I , where the response is ohmic, and disappear at higher I (SLCO sample A in B^\perp). (b) The magnetic field indicated by both the Hall sensor and electromagnet current produce comparable oscillations. Also these curves were measured by hand in a completely manual fashion without computer intervention. (c) This curve was measured with a pulsed current and still shows oscillations.

that the low- I $R(B)$ curves of Fig. 5(a) overlap and show independence of I and V over a sevenfold range. This indicates a perfect ohmic I - V response, whereas the presence of weak links and microwave radiation would have lead to Shapiro steps in the I - V response [29]. In fact the entire range of effects related to weak links and noise, is incapable of producing such $R(B)$ oscillations with a ΔB independent of T and geometry.

Figure 5(b) shows $R(B)$ curves with the abscissa taken in two ways: one uses the B measured by the Hall sensor and the other is the B estimated from the electromagnet current. Notwithstanding the small disagreement and offset in B (expected from the hysteresis and nonlinear response of the magnet's iron core), the oscillations are reproduced by both methods and are therefore not an artifact of the B measurement. Furthermore the curves in Fig. 5(b) were measured with a different voltmeter (a Keithley 2000 multimeter instead of the 2182A nanovoltmeter) and were measured completely manually, to rule out any possible artifacts from a computer controlled data acquisition system.

A final test, shown in Fig. 5(c), demonstrates that the oscillations can also be seen in a pulsed transport measurement (involving an entirely different chain of electronics), if care is taken to minimize the introduction of spurious noise (careful isolation of the pulse generator and amplifiers from the mains power using isolation transformers and capacitors). In light of these extensive cross-checks using multiple instruments (three thermometers, three voltmeters, three current sources, and two B measurements) we were not able to associate these oscillatory features to any artifact that could be produced

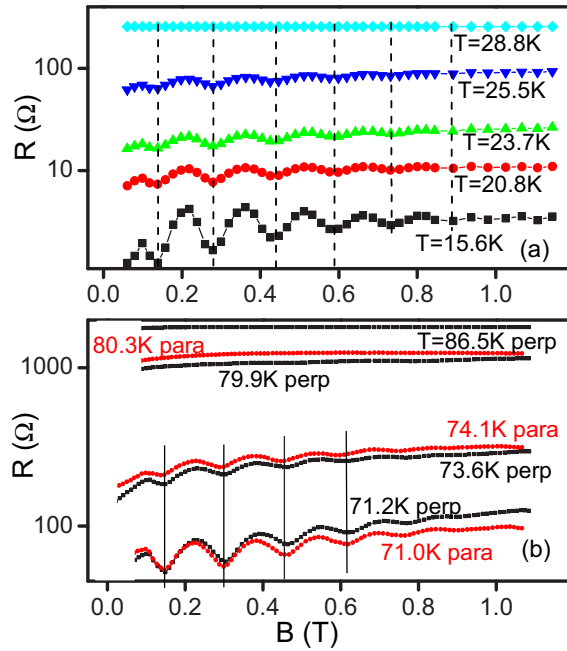


FIG. 6. (a) B^{\parallel} oscillatory magnetoresistance in SLCO sample B. (b) B^{\parallel} and B^{\perp} oscillatory magnetoresistance in YBCO.

by the apparatus, therefore proving that it is an intrinsic phenomenon.

Figure 6 shows oscillatory $R(B)$ curves for the other SLCO sample B (with very different dimensions) and the YBCO sample. Note that YBCO is a hole-doped cuprate superconductor unlike the electron-doped SLCO, and has a three times higher T_c . Incredibly, these other samples have periodicities ($\Delta B = 0.147 \pm 0.007$ T and 0.150 ± 0.004 T, respectively) that are identical to the first SLCO sample within their error bars. Additionally we have also observed OMR in the $\text{Nd}_{2-x}\text{Ce}_x\text{CuO}_4$ electron-doped cuprate superconductor and in the $\text{Bi}_2\text{Te}_3/\text{FeTe}$ topological-insulator/iron-chalcogenide

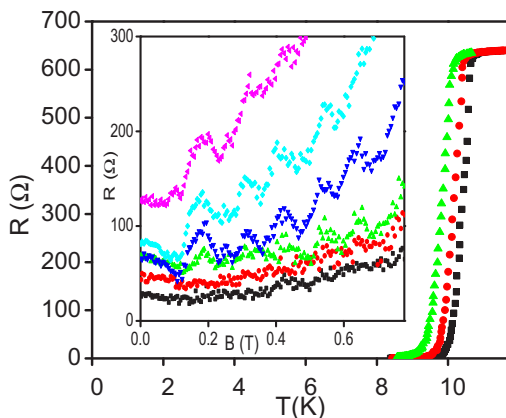


FIG. 7. Resistive transitions of a NbTiN superconducting film in parallel magnetic fields (right to left) of $B^{\parallel} = 0, 0.63,$ and 1.12 T in $I = 115 \mu\text{A}$. The inset shows B^{\parallel} oscillatory magnetoresistance in the foot region of the transitions, which only appears at a very low current of $I = 97$ nA; the temperatures of the curves (bottom to top) are $T = 9.51, 9.57, 9.71, 9.87, 10.00,$ and 10.14 K.

interfacial superconductor with similar ΔB periods (0.14 and 0.11 T) despite their different material parameters and dimensions; those results will be described in detail elsewhere. Not all superconducting samples show the phenomenon and it is not known what induces OMR in some samples but not in others. In some cases the OMR only appears at very low current densities j , such as in the NbTiN sample whose data are shown in Fig. 7. Despite being a conventional superconductor with a relatively sharp transition, at a sufficiently low $j \sim 10$ A/cm², OMR with $\Delta B \approx 0.12$ T is discernible despite the low signal-to-noise ratio (a consequence of the low current).

IV. DISCUSSION

Since this OMR phenomenon is most easily seen within the resistive transition, one might be inclined to associate the phenomenon with inhomogeneity or granularity; however, we show below that it is more likely that the OMR is fundamentally unrelated to the disorder but that a wider transition helps to make the oscillations more conspicuous: with a perfectly sharp transition, the system would switch too abruptly from zero resistance to the normal state to show oscillations (even the original Little Parks effect would be invisible if the transition were perfectly sharp as discussed by Tinkham [30]). Nevertheless let us explore how granularity and a weak-linked structure might produce OMR. Oscillations can arise from fluxoid quantization if the system is multiply connected. A granular material can potentially have percolating loops that could enclose flux; as the enclosed flux changes in steps of Φ_0 with increasing applied B , the supercurrent I_s around the loop will oscillate to keep the fluxoid Φ' quantized to ensure that the phase is single valued at any point around the loop. In doing so, the order parameter is suppressed when I_s is on a maximum. At certain values of T and B , this maximum current may drive some weak links in the loop resistive, leading to a periodic variation in resistance with a period $\Delta B \approx \Phi_0/S$. If such loops form randomly through coupling of nearby grains, one would expect that the geometry of the coupled structures would change with T and B . Also one would expect there to be a multiplicity of loop sizes and therefore a superposition of periods, whereas we find only one prominent period in the FFT spectrum that is independent of all parameters. There is also the matter of the loop size, which would have to have the area $S = \Phi_0/\Delta B \approx 117^2$ nm² transverse to the field for our observed $\Delta B \approx 0.15$ T. This dimension is smaller than the film thickness in one case, but much larger than d in other cases. How does one address the B^{\parallel} case when $d \ll 117$ nm? By taking $d \times l$ as the effective area? The two SLCO samples with identical periods had $d \times l = 3400^2$ and 2500^2 nm², both much larger than the required 117^2 nm². For the loop theory to work, somehow the length of the bridge will have to be broken up into segments of length l' such that $d \times l' \approx 117^2$ nm². For our range of thicknesses, this would imply $l' = 59$ – 2700 nm to magically produce the same constant $d \times l' \approx 117^2$ nm². There is no evidence to support such a segmentation. Therefore, a possible explanation for oscillations along these lines is probably not valid, as also noted by others [27,31].

Aside from well connected loops leading to Little Parks like oscillations, Josephson junctions can lead to oscillatory

interference effects and granular systems can surely have junctions between grains. A single junction can itself produce OMR because of the Fraunhofer pattern in the functional dependence between the maximum supercurrent it can carry and the flux linking the junction: $I_m(B) = I_m(0)|\sin(\pi\Phi/\Phi_0)/(\pi\Phi/\Phi_0)|$. Minima in $I_m(B)$ will correspond to maxima in $R(B)$ with a periodicity in linked flux of Φ_0 . For a junction with parallel faces and a rectangular cross section (of separation D and length L) transverse to B , the linked flux is $\Phi = BL(D + 2\lambda)$, where λ is the magnetic penetration depth. This leads to the requirement $L(D + 2\lambda) \approx 117^2 \text{ nm}^2$ for the observed $\Delta B = 0.15 \text{ T}$. However, there are two problems with this: first, λ varies with T , so ΔB would not be T independent and, second, the linked area and hence ΔB would depend on the orientation of B . Furthermore, the neat Fraunhofer pattern becomes replaced by a more general Fourier transform if the junction is not rectangular or has a variation in the local critical current density over the face of the junction. Add to this the complexity of having a spread in junction sizes and characteristics in a random granular system and it becomes clear that the single junction diffraction pattern is not a viable candidate for the type of OMR discussed in this work.

We next consider closed paths containing multiple JJs, taking first the simplest case of a two-junction loop in which the junctions themselves are small enough to have negligible single-junction diffraction effects. The net current entering and leaving the loop is the phase sensitive summation of the currents through the two junctions. The supercurrent through each JJ is given by $I_s = I_c \sin \gamma$, where γ is the gauge invariant phase difference across the junction and I_c is the JJ critical current (above which resistance appears). Since the net phase difference going around the loop must be single valued, we have $\gamma_1 - \gamma_2 = 2\pi\Phi/\Phi_0 \pmod{2\pi}$. Thus the two JJs can carry their maximum critical currents (when $\gamma_1 = \gamma_2 = \pi/2$) when Φ is an integer multiple of Φ_0 once again leading to the periodicity $\Delta B = \Phi_0/S$; however, if there are more than two JJs in the loop, or if the loops have different areas, or if the junctions themselves have appreciable flux linkage to exhibit their own diffraction effects, a single well defined periodicity will not exist. Thus a granular system, unless it is so small that it includes only a few grains, will not have oscillations with a single clearly defined period. This was exactly the observation by Herzog *et al.*, who found that their granular tin films did not display any oscillations unless patterned down to extremely small nanowires, and even then contained a superposition of multiple periods. The epitaxial films in our work show OMR irrespective of the bridge size and field orientation. In fact our bridges are seven orders of magnitude greater in volume than the nanowires in some of these other works, yet we see clean single-period OMR. Such an extended system will only have fluxoid/vortex based clear OMR if it is purposely patterned with a regular array as in Ref. [26]. It seems impossible for the bridge to accidentally and coincidentally have loops of 117^2 nm^2 when the area of the bridge facing the field is 10^{11} nm^2 .

The formation and motion of vortices—and the interplay between the applied magnetic field, thermal excitations, and the self-field of the current—provides yet another basis for OMR. Modulations in the barriers at the sample edges for entry/exit of vortices lead to changes in the static and dynamic

phases of the vortex matter. This in turn can lead to alternations in the dissipation even in singly connected superconducting strips. These ideas were proposed by Anderson and Dayton [32], and elaborated upon by Sochnikov *et al.* [22] and Berdiyrov *et al.* [24]. More recently, Berdiyrov *et al.* [33] performed a careful Ginzburg-Landau study with numerical simulations of these regimes for the B^\perp case; they found that the qualitative nature and period of the OMR depended on the strip width and the amount of disorder. Indeed this variability of ΔB in vortex based OMR was reported in even the earliest experiments by Parks and Mochel [34,35]. Thus this class of vortex-based effects cannot explain the nearly constant ΔB observed in the present work. For B close to B^\parallel , rearrangements of the parallel vortex system [36] provide another mechanism for oscillations; however, the positions of the peaks depend on the field tilt angle, whereas the present oscillations don't depend on the angle and even occur for B^\perp .

Finally, to cover other known origins of OMR, the Fulde-Ferrell-Larkin-Ovchinnikov (FFLO) modulated superconducting state [37,38] could result in oscillations if its wave vector $q \sim 2\mu_B B/(\hbar v_F)$ (in the microns range) matches some intrinsic spatial periodicity, but this doesn't match any known length scale in our systems, and the ΔB would be expected to depend on the material and the dimensions. Furthermore the present films do not have the special characteristics (e.g., clean, appropriate nesting of Fermi surfaces, etc.) that favor FFLO formation. The Shubnikov-de Haas effect [39] is another scenario that produces OMR; however, these are periodic in $1/B$, rather than in B , and occur at very high values $B \gg 1 \text{ T}$. All of the above effects depend on the orientation of B , material parameters (Fermi-surface geometry, Fermi velocity, coherence length, etc.), and/or sample dimensions and geometry. Thus the previously established mechanisms that we are aware of cannot straightforwardly explain the observed nearly universal periodicity.

So what other physical mechanisms might underlie the oscillations? In the dissipative state of a superconductor, resistance rises—whether the current is flowing through the bulk or percolating across junctions—when the superconducting state is weakened, signaled by a reduction in the order parameter Δ . Thus minima in $R(B)$ may be assumed to reflect values of B where there are peaks in Δ . Δ can rise because of an increase in the strength of the attractive pairing interaction, an increase in the density of states (DOS) at the Fermi level, or a reduction of pair breakers that interfere with the pairing. We are not aware of any mechanism by which B could directly alter the fundamental pairing attraction. However, B can affect the DOS and it certainly causes pair breaking. A magnetic field weakens the superconducting state in two main ways: through orbital pair breaking and through Pauli paramagnetism. The former, both in the mixed state and the fluctuation regime [40], is highly material, temperature, and field-orientation dependent, so we reject the role of this component. The paramagnetic effect, on the other hand, leads to an energy splitting $\Delta E_p = \pm\mu_B \Delta B \approx \pm 9 \mu\text{eV}$ (for the observed $\Delta B \approx 0.15 \text{ T}$) between opposite spins, which is indeed universal and not dependent on the material or other parameters (here $\mu_B = e\hbar/2m$ is the Bohr magneton). Normally this would lead to a progressive weakening of Δ and a monotonic rise in R with increasing B . However, there are two ways by which Δ could be strengthened

by B as follows. (1) One is if the DOS is a nonmonotonic function of energy, e.g., if the ΔE_p pushed the Fermi level for one of the spin directions into the vicinity of a peak in the DOS, then the field could actually strengthen the superconducting state. For multiple oscillatory periods, one would need a “comb” in the DOS. (2) The second route is if ΔE_p canceled a preexisting pair breaker which had a higher energy for spin-up versus spin-down states, in which case the ΔE_p would reduce the net pair breaking by bringing the energies of time reversed states into alignment and thereby strengthen the superconducting state. (An example of a situation where a spin-up state has a higher intrinsic energy than a spin-down state, is the $2S_{1/2}-2P_{1/2}$ [equal total angular momentum] pair of states in a singular attractive potential, whose degeneracy is lifted because of QED radiative corrections from interactions with the vacuum; in the context of an atom, this process is manifested as the familiar Lamb shift, which is of the order of $10 \mu\text{eV}$.) At the present time, it is not clear whether either of these mechanisms have any relevance to the observed phenomenon, or how they would lead to multiple oscillation periods beyond a single dip in R . The ideas are only suggested as possible directions for exploring explanations.

V. SUMMARY AND CONCLUSIONS

We have observed periodic oscillations in magnetoresistance at low fields ($B \sim 0-1$ T) with a period that is independent of temperature, magnetic field, electric transport current, and even the orientation of the magnetic field. Moreover, the period doesn't vary much even across different materials. Collectively, between our measurements and the earlier cited work, a very wide range of materials (from lead to cuprates) are covered. The different films were made with almost every possible method of deposition (from thermal and electron-beam evaporation to MBE) and patterned into bridges/wires by a multitude of techniques (focused ion-beam lithography, shadow masking, resist based lithography with chemical etching as well as ion milling, etc.). The sample sizes span many orders of magnitude for each dimension:

$d = 7-250$ nm, $w = 0.1-50 \mu\text{m}$, and $l = 1-2000 \mu\text{m}$, and have a variety of geometries and lead arrangements. This OMR has been observed at temperatures ranging from 12 mK to 74 K, and these measurements were conducted using a variety of cryogenic systems, which include a closed-cycle cryocooler (the present work), a Quantum Design Physical Properties Measurement system [27], and even a helium-3 cryostat and dilution refrigerator [28]. Yet the periods span a rather narrow range: all three cuprate materials have a period of 0.15 ± 0.01 T, the conventional low- T_c film has a period of 0.12 T, and our interfacial superconductor has a period of 0.11 T. The earlier observations of similar low-field periodic OMR in conventional low- T_c materials also have comparable periods of $\Delta B = 0.12, 0.13,$ and 0.18 T. To our knowledge and understanding, it is hard to reconcile this magnitude and near universality of period with models invoking vortices, fluxoid quantization, and Josephson-junction type of effects. It seems that the oscillations also cannot originate from Fermi-surface based microscopic phenomena that are known to cause OMR. Thus, while it may still be possible to explain our observations through some intricate or exotic modifications of the known aforementioned mechanisms, the results also indicate the possibility that a potentially new phenomenon might be operative and some suggestions were made in the text as to possible directions for pursuing an explanation. We hope that our observations and information will stimulate further experimental and theoretical investigations into this phenomenon.

ACKNOWLEDGMENTS

The authors would like to thank the following for providing samples, useful discussions, and other assistance: L. Fruchter, Z. Z. Li, M. Liang, J. M. Knight, N. S. Moghaddam, S. Varner, R. A. Webb, K. Stephenson, N. Lu, and M. Geller. This work was supported by the U. S. Department of Energy, Office of Science, Office of Basic Energy Sciences, under Grant No. DE-FG02-99ER45763. B.I.I. acknowledges support from CONACYT through Grant No. 237439.

-
- [1] W. A. Little and R. D. Parks, *Phys. Rev. Lett.* **9**, 9 (1962); R. D. Parks and W. A. Little, *Phys. Rev.* **133**, A97 (1964).
 - [2] J. Bardeen, *Phys. Rev. Lett.* **7**, 162 (1961).
 - [3] R. P. Groff and R. D. Parks, *Phys. Rev.* **176**, 567 (1968).
 - [4] H. J. Fink, A. Lopez, and R. Maynard, *Phys. Rev. B* **26**, 5237 (1982).
 - [5] J. Simonin, D. Rodrigues, and A. Lopez, *Phys. Rev. Lett.* **49**, 944 (1982).
 - [6] R. M. Arutunian and G. F. Zharkov, *J. Low Temp. Phys.* **52**, 409 (1983).
 - [7] R. Rammal, T. C. Lubensky, and G. Toulouse, *Phys. Rev. B* **27**, 2820 (1983).
 - [8] J. M. Gordon, A. M. Goldman, and B. Whitehead, *Phys. Rev. Lett.* **59**, 2311 (1987).
 - [9] F. Nori and Q. Niu, *Physica B* **152**, 105 (1988).
 - [10] J. M. Gordon and A. M. Goldman, *Physica B* **152**, 125 (1988).
 - [11] P. L. Gammel, P. A. Polakos, C. E. Rice, L. R. Harriott, and D. J. Bishop, *Phys. Rev. B* **41**, 2593 (1990).
 - [12] O. Buisson, M. Giroud, and B. Pannetier, *Europhys. Lett.* **12**, 727 (1990).
 - [13] H. Vloeberghs, V. V. Moshchalkov, C. Van Haesendonck, R. Jonckheere, and Y. Bruynseraede, *Phys. Rev. Lett.* **69**, 1268 (1992).
 - [14] C. C. Chi, P. Santhanam, and P. E. Blochl, *Phys. Rev. B* **42**, 76 (1990).
 - [15] V. V. Moshchalkov, L. Gielen, M. Dhalle, C. Van Haesendonck, and Y. Bruynseraede, *Nature (London)* **361**, 617 (1993); V. V. Moshchalkov, L. Gielen, C. Strunk, R. Jonckheere, X. Qiu, C. Van Haesendonck, and Y. Bruynseraede, *ibid.* **373**, 319 (1995).
 - [16] J. I. Castro and A. Lopez, *Phys. Rev. B* **52**, 7495 (1995).
 - [17] A. G. Sivakov, A. M. Glukhov, A. N. Omelyanchouk, Y. Koval, P. Müller, and A. V. Ustinov, *Phys. Rev. Lett.* **91**, 267001 (2003).

- [18] O. Sato and M. Kato, *Phys. Rev. B* **68**, 094509 (2003).
- [19] M. D. Stewart, Jr., Z. Long, J. M. Vallas, Jr., A. Yin, and J. M. Xu, *Phys. Rev. B* **73**, 092509 (2006).
- [20] U. Patel, Z. L. Xiao, J. Hua, T. Xu, D. Rosenmann, V. Novosad, J. Pearson, U. Welp, W. K. Kwok, and G. W. Crabtree, *Phys. Rev. B* **76**, 020508 (2007).
- [21] G. R. Berdiyrov, S. H. Yu, Z. L. Xiao, F. M. Peeters, J. Hua, A. Imre, and W. K. Kwok, *Phys. Rev. B* **80**, 064511 (2009); G. R. Berdiyrov, M. V. Milosevic, and F. M. Peeters, *ibid.* **81**, 144511 (2010).
- [22] I. Sochnikov, A. Shaulov, Y. Yeshurun, G. Logvenov, and I. Bozovic, *Nat. Nanotechnol.* **5**, 516 (2010); *Phys. Rev. B* **82**, 094513 (2010).
- [23] J. R. Kirtley, C. C. Tsuei, V. G. Kogan, J. R. Clem, H. Raffy, and Z. Z. Li, *Phys. Rev. B* **68**, 214505 (2003).
- [24] G. R. Berdiyrov, M. V. Milosevic, M. L. Latimer, Z. L. Xiao, W. K. Kwok, and F. M. Peeters, *Phys. Rev. Lett.* **109**, 057004 (2012).
- [25] A. V. Herzog, P. Xiong, and R. C. Dynes, *Phys. Rev. B* **58**, 14199 (1998).
- [26] H. S. J. van der Zant, M. N. Webster, J. Romijn, and J. E. Mooij, *Phys. Rev. B* **50**, 340 (1994).
- [27] J. Wang, X. Ma, S. Ji, Y. Qi, Y. Fu, A. Jin, L. Lu, C. Gu, X. C. Xie, M. Tian, J. Jia, and Q. Xue, *Nano Res.* **2**, 671 (2009).
- [28] A. Johansson, G. Sambandamurthy, D. Shahar, N. Jacobson, and R. Tenne, *Phys. Rev. Lett.* **95**, 116805 (2005).
- [29] S. Shapiro, *Phys. Rev. Lett.* **11**, 80 (1963).
- [30] M. Tinkham, *Introduction to Superconductivity*, 2nd ed. (McGraw-Hill, New York, 1996).
- [31] J. Wang, X. Ma, L. Lu, A. Jin, C. Gu, X. C. Xie, J. Jia, X. Chen, and Q. Xue, *Appl. Phys. Lett.* **92**, 233119 (2008).
- [32] P. W. Anderson and A. H. Dayem, *Phys. Rev. Lett.* **13**, 195 (1964).
- [33] G. R. Berdiyrov, X. H. Chao, F. M. Peeters, H. B. Wang, V. V. Moshchalkov, and B. Y. Zhu, *Phys. Rev. B* **86**, 224504 (2012).
- [34] R. D. Parks and J. M. Mochel, *Phys. Rev. Lett.* **11**, 354 (1963).
- [35] R. D. Parks and J. M. Mochel, *Rev. Mod. Phys.* **36**, 284 (1964).
- [36] S. H. Brongersma, E. Verweij, N. J. Koeman, D. G. de Groot, R. Griessen, and B. I. Ivlev, *Phys. Rev. Lett.* **71**, 2319 (1993).
- [37] P. Fulde and R. A. Ferrell, *Phys. Rev.* **135**, A550 (1964).
- [38] A. I. Larkin and Yu. N. Ovchinnikov, *Sov. Phys. JETP* **20**, 762 (1965).
- [39] A. A. Abrikosov, *Fundamentals of the Theory of Metals* (North-Holland, Amsterdam, 1988).
- [40] A. Larkin and A. Varlamov, *Theory of Fluctuations in Superconductors* (Oxford Science Publications, Oxford, 2005).